

# Electron Spin Resonance and Electron Spin Echo Modulation Studies of *N,N,N',N'*-Tetramethylbenzidine Photoionization in Anionic Micelles: Structural Effects of Tetramethylammonium Cation Counterion Substitution for Sodium Cation in Dodecyl Sulfate Micelles

E. Szajdzinska-Piętek,<sup>††</sup> René Maldonado,<sup>‡</sup> Larry Kevan,<sup>\*†</sup> and Richard R. M. Jones<sup>§</sup>

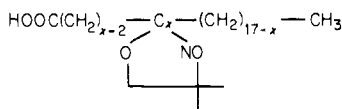
Contribution from the Departments of Chemistry, University of Houston, Houston, Texas 77004, and Wake Forest University, Winston-Salem, North Carolina 27109.

Received December 6, 1983

**Abstract:** Comparative electron spin resonance and electron spin echo modulation studies have been carried out for the radical cation produced by photoionization of *N,N,N',N'*-tetramethylbenzidine in micellar sodium dodecyl sulfate (SDS) and tetramethylammonium dodecyl sulfate (TMADS) solutions. It is found that the substitution of tetramethylammonium ion for sodium ion brings about a marked increase in photoionization efficiency at 77 K which correlates with increased photoproduced cation-water interactions as determined by electron spin echo modulation (ESEM) experiments. ESEM experiments have also been performed for a series of *x*-doxylstearic acids as paramagnetic probes in both micellar solutions. The data indicate more water penetration in TMADS than in SDS micelles. The results have been explained in terms of a decrease in the compactness of the micelle polar head-group region and increased surface roughness by the substitution of the more hydrophobic tetramethylammonium cation for sodium cation.

Micellar solutions are widely used as models for artificial photosynthetic systems. Photoionization and charge separation processes in these organized molecular assemblies may be markedly affected by structural factors, such as micelle size and shape, and the location of the photoionizable molecule with respect to the micellar surface.<sup>1</sup> The structural location and water interactions of photoproduced *N,N,N',N'*-tetramethylbenzidine (TMB) cation in various frozen micellar systems were studied recently in this laboratory by means of electron spin resonance (ESR) and electron spin echo modulation (ESEM) methods.<sup>2,3</sup> Photoproduced cation-water interactions detected by ESEM in micelles of sodium alkyl sulfates have been found to increase with decreasing alkyl chain length. This was interpreted as consistent with an asymmetric solubilization site for TMB molecule near the micellar surface and with little water penetration into the micelle. Furthermore, in frozen alkyl sulfate solutions the yield of photoproduced TMB<sup>+</sup> was found to correlate with increased TMB<sup>+</sup>-water interactions.<sup>3</sup>

In the present work we have carried out similar investigations for tetramethylammonium dodecyl sulfate (TMADS) micellar solution to compare the results with those for sodium dodecyl sulfate (SDS). On the basis of the reported counterion specificity in the formation of ionic micelles<sup>4,5</sup> it was anticipated that the exchange of a hydrophilic counterion for a hydrophobic one would affect the photoionization efficiency and the cation-water interactions. In addition to the experiments with TMB in micelles, we have made ESEM studies using a series of *x*-doxylstearic acid spin probes with the structure given by



where *x* was equal to 5, 7, and 10. By monitoring the nitroxide-water interactions as a function of doxyl group position, we have been able to obtain information about the degree of water penetration into the micellar core.

## Experimental Section

SDS and TMB from Eastman Kodak Co., Kodak Laboratory and Specialty Chemicals, as well as the doxylstearic acids from Molecular

Probes, Inc., were used as obtained. SDS from British Drug Houses Ltd. was also used in some experiments with identical results. TMADS was prepared as follows. Dodecanoic acid (Matheson, Coleman and Bell, lauric acid) was esterified with ethyl alcohol in benzene by using concentrated sulfuric acid catalyst and azeotropic distillation of water. The extracted (ether), washed (saturated NaCl, saturated NaHCO<sub>3</sub>), and dried (anhydrous MgSO<sub>4</sub>) product was distilled, accepting the fraction boiling at 143–143.5 °C at 10 torr. Gas chromatographic analysis (12 ft × 1/8 in. 8% SP1000, 175 °C and 6 ft × 1/8 in. 3% Dexil 300, 150 °C, Perkin-Elmer Sigma 3, flame ionization detection) showed this material to be free of impurities of shorter or longer chain length. Lithium aluminum tetrahydride (LAH, Aldrich, 95+%) reduction of the ester in dry diethyl ether (from LAH) using a twofold excess of hydride and reflux after the addition yielded the alcohol. The hydrolyzed (1 N HCl), extracted (ether), washed (saturated NaCl, saturated NaHCO<sub>3</sub>), and dried (Na<sub>2</sub>SO<sub>4</sub>) dodecanol was distilled, accepting the fraction boiling at 118–118.5 °C at 3.2 torr. Gas chromatographic analysis (6 ft × 1/8 in. 8% SP1000, 175 °C) showed no contamination by the ester and no other alcohol above 0.1%. Ten milliliters (10.2 g, 0.0546 mol) of this material was sulfated with an equimolar quantity of freshly distilled chlorosulfonic acid (3.65 mL, 0.0553 mol, bp 151–152 °C, laboratory atmosphere pressure, Fisher Purified Grade, lit. 158 °C) by slow addition of the acid by syringe to a dry diethyl ether (50 mL anhydrous, Fisher, ACS grade) solution of the alcohol contained in a 100-mL round-bottom flask equipped with a magnetic stir bar and a Neoprene rubber septum, under dry nitrogen, and cooled in an ice bath. After the solution was warmed to room temperature and stirred for 1 h, it was poured onto 50 g of ice in a separatory funnel. Butanol (60 mL, Fisher HPLC grade) was added and the aqueous layer extracted, with a Teflon stopcock separatory funnel to avoid grease. The aqueous layer was further extracted twice with 30-mL portions of butanol, and the combined butanol extractions were washed three times with water to remove sulfuric acid. The butanol layer was neutralized with 48 mL of a 10% aqueous solution of tetramethylammonium hydroxide (Matheson, Coleman and Bell) to pH 7. The butanol was then evaporated on a rotary evaporator at 50 °C until crystals formed. A fresh 50 mL of dry butanol was added, the crystals were dissolved by heating to 50 °C, and the evaporation was continued to remove the water. The evaporation was terminated at the first sign of cloudiness and the material hot filtered to remove tetra-

(1) See, for example: (a) Thomas, J. K. *Acc. Chem. Res.* **1977**, *10*, 133. (b) Calvin, M. *Ibid.* **1978**, *11*, 369. (c) Fendler, J. H. *J. Phys. Chem.* **1980**, *84*, 1485.

(2) Narayana, P. A.; Li, A. S. W.; Kevan, L. *J. Am. Chem. Soc.* **1981**, *103*, 3603.

(3) Narayana, P. A.; Li, A. S. W.; Kevan, L. *J. Am. Chem. Soc.* **1982**, *104*, 6502.

(4) Mukerjee, P.; Mysels, K. J.; Kapauan, P. J. *J. Phys. Chem.* **1976**, *71*, 4166.

(5) Almgren, M.; Swarup, S. *J. Phys. Chem.* **1983**, *87*, 876.

<sup>††</sup> On leave from the Institute of Applied Radiation Chemistry, Technical University of Łódź, Poland.

<sup>‡</sup> University of Houston.

<sup>§</sup> Wake Forest University.

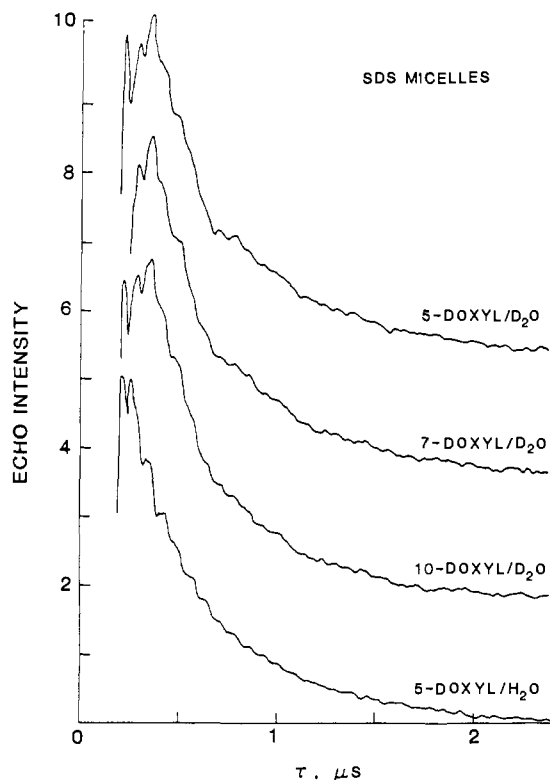


**Figure 1.** Two-pulse electron spin echo decay curves at 4.2 K of  $\alpha$ -doxylstearic acid probes in SDS micelles prepared in  $D_2O$  and in  $H_2O$  as indicated. The base lines have been offset vertically to avoid overlap. The maxima of each decay curve are normalized to the same value.

methylammonium sulfate. Upon cooling, the butanol deposited white needles of the tetramethylammonium dodecyl sulfate (TMADS). These were collected and recrystallized four times from absolute ethanol (U.S. Industrial Chemicals Co., U.S.I. pure ethyl alcohol, dehydrated, U.S.P.) to remove traces of butanol. The product was dried to constant weight under vacuum at room temperature. Anal. (Galbraith Laboratories, Inc., Knoxville, TN). Found: C, 56.71; H, 11.14; N, 4.08; S, 9.55. Calcd: C, 56.60; H, 10.98; N, 4.13; S, 9.44.

Surfactant solutions (0.1 M) were prepared in triply distilled  $H_2O$  for ESR studies or in  $D_2O$  from Aldrich Chemical Co. for ESEM studies. Water was deoxygenated by nitrogen bubbling and samples were prepared in a nitrogen atmosphere. TMB and doxylstearic acid probes were solubilized in micellar solutions by the procedures described previously<sup>3,6</sup> to a concentration of ca. 0.3 and 0.4 mM, respectively. In solutions used for studies of photoionization efficiency, the TMB concentration determined by absorption measurements at 306 nm, using an extinction coefficient of  $3.4 \times 10^4 \text{ M}^{-1} \text{ cm}^{-1}$ , was carefully adjusted to the same value for both surfactants by dilution with the proper stock solutions.

The samples were sealed in 2-mm o.d. Suprasil quartz tubes for the ESR studies and in 3-mm o.d. Suprasil quartz tubes for the ESEM studies and were frozen in 2–3 s by plunging them into liquid nitrogen. The TMB samples were irradiated with  $370 \pm 40 \text{ nm}$  light using a high-pressure mercury lamp and a Corning 7–60 filter to give a flux of  $1 \times 10^2 \text{ W m}^{-2}$ . ESR spectra were recorded on a Varian E-4 spectrometer. The two-pulse electron spin echo signals were recorded at 4.2 K on a home-built spectrometer.<sup>7</sup> Measurements were done at  $\sim 9.15 \text{ GHz}$ , and the width of the exciting pulses was 50 ns. The data were transmitted to a Tektronix 4052 computer which normalized the maxima of all the spin echo decay curves to the same value. A Cary-14 spectrophotometer was used to measure the TMB optical absorption spectra.

## Results

**ESEM Studies of Water–Nitroxide Probe Interactions.** Two-pulse electron spin echo decay curves for 5-, 7-, and 10-doxylstearic acid probes in micellar solutions prepared in  $D_2O$  are presented in Figures 1 and 2 for SDS and TMADS, respectively. The results for 5-doxylstearic acid in  $H_2O$  micellar solutions are also included for comparison. The data were recorded at 4.2 K from the  $M_I=0$

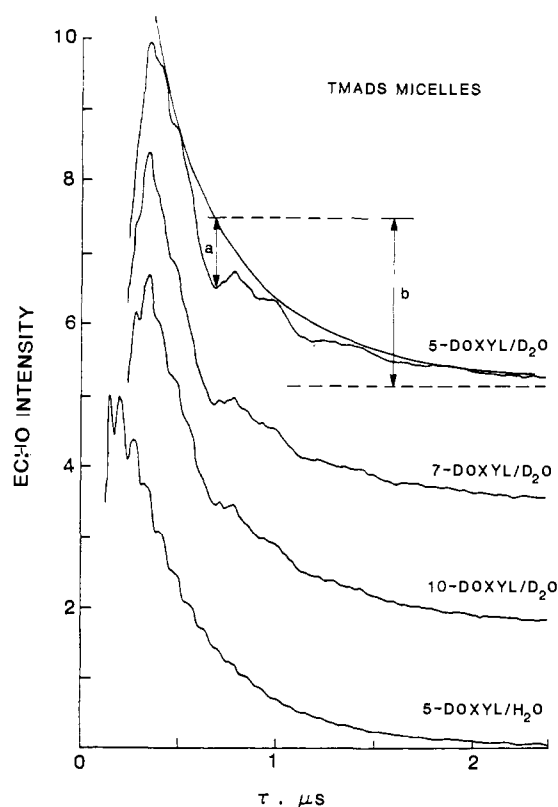


**Figure 2.** Two-pulse electron spin echo decay curves at 4.2 K of  $\alpha$ -doxylstearic acid probes in TMADS micelles prepared in  $D_2O$  and in  $H_2O$  as indicated. The base lines have been offset vertically to avoid overlap and the maxima of each decay curve are normalized to the same values. The normalized modulation is defined as  $a/b$ .

$^{14}\text{N}$  hyperfine transition of the nitroxide ESR spectrum. The echo intensity decreases with time,  $\tau$ , between the two applied microwave pulses and the decay curves exhibit periodic modulations due to weak electron–nuclear hyperfine interactions between the nitroxide probe and the nearby magnetic nuclei. In the applied field, the  $0.08\text{-}\mu\text{s}$  modulation period corresponds to electron–proton interactions, while the  $0.5\text{-}\mu\text{s}$  modulation period corresponds to electron–deuteron interactions.<sup>8</sup>

Proton modulation is observed in all the samples and arises due to nitroxide probe interactions with protons on the surfactant molecules. For  $D_2O$  solutions deuterium modulation can also be seen which corresponds to interactions of the spin probe with water molecules. As shown in Figures 1 and 2 this modulation is superimposed on the echo decay.<sup>8</sup> The normalized modulation can be determined as defined in Figure 2, as the depth from the unmodulated extrapolation divided by the unmodulated echo signal at that interpulse time. The trends in the data are plotted in Figure 3 and represent at least duplicate experiments.

**ESEM Studies of Water–TMB<sup>+</sup> Interactions.** Two-pulse electron spin echo spectra recorded at 4.2 K for TMB cation in TMADS and SDS micellar  $D_2O$  solutions are shown in Figure 4. Here again one can see distinct deuterium modulation in addition to the proton modulation. The deuterium modulation depth is rather small in SDS, as observed previously,<sup>3</sup> but it is distinctly larger in TMADS, indicating stronger TMB cation–water interactions.

**ESR Studies of TMB Photoionization Efficiency.** After 240-s irradiation with 370-nm light at room temperature, typical ESR spectra of TMB cation were observed<sup>2</sup> with the intensity in TMADS micellar solutions being about 0.7 of that in SDS micellar solutions. The quantum yield of TMB<sup>+</sup> in SDS micelles is about 0.04 near pH 7. The photoproducted TMB cation is unstable and decays somewhat faster in TMADS than in SDS micelles, as

(6) Bales, B. L.; Kevan, L. *J. Phys. Chem.* **1982**, *86*, 3836.

(7) Ichikawa, T.; Kevan, L.; Narayana, P. A. *J. Phys. Chem.* **1979**, *83*, 3378.

(8) Kevan, L. In "Time Domain Electron Spin Resonance"; Kevan, L., Schwartz, R. N., Eds.; Wiley-Interscience: New York, 1979; Chapter 8.

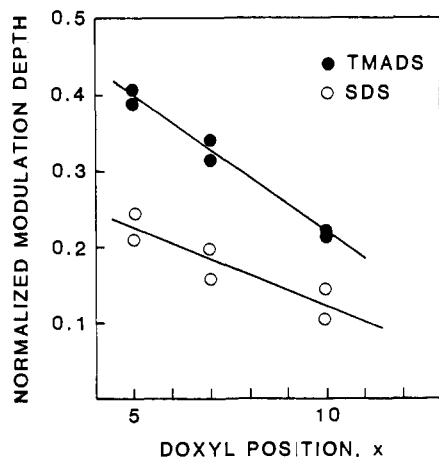


Figure 3. Normalized ESE modulation depth of *x*-doxyl stearic acid in 0.1 M TMADS and 0.1 M SDS micelles in D<sub>2</sub>O.

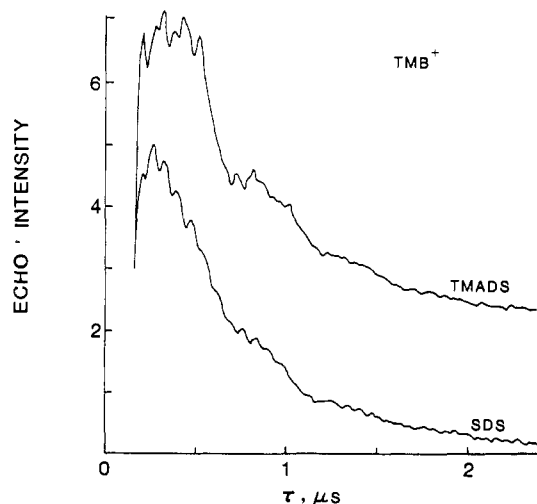


Figure 4. Two-pulse electron spin echo decay curves at 4.2 K of photogenerated TMB<sup>+</sup> in TMADS and SDS micelles prepared in D<sub>2</sub>O. The base lines have been offset vertically to avoid overlap and the maxima of each decay curve are normalized to the same value.

shown in Figure 5. In both cases the decay can be characterized by two concomitant first-order processes. Analysis gives rate constants of  $3.2 \times 10^{-4}$  and  $4.0 \times 10^{-4} \text{ s}^{-1}$  for the slow decay of TMB<sup>+</sup> in SDS and TMADS micelles, respectively. Subtraction of this slow decay from the remaining faster decay at short times gives a linear semilogarithmic plot with rate constants of  $4.9 \times 10^{-3}$  and  $8.5 \times 10^{-3} \text{ s}^{-1}$  for SDS and TMADS micelles, respectively. Alternatively, the decay can be interpreted in terms of a time-dependent rate constant.<sup>9</sup>

Thus, the difference in room temperature steady-state concentrations of TMB<sup>+</sup> in TMADS as compared to SDS reflects the shorter cation lifetime in TMADS. On the other hand, TMB<sup>+</sup> photoproduced at 77 K does not decay during hours and gives the ESR spectra in Figure 6. Because a different line shape is observed in frozen TMADS micellar solutions compared to frozen SDS micellar solutions, a double integration procedure was used to estimate the relative TMB<sup>+</sup> concentrations. After the same irradiation time, 480 s, the concentration in TMAS is 1.6 higher than in SDS, indicating a higher photoionization efficiency in TMADS micellar solutions at 77 K.

We note that there could be some structural distortion on freezing the micellar solutions; however, previous experiments have shown that the micellar structure is retained.<sup>2</sup> Similar results for TMADS vs. SDS micellar solutions in liquid and frozen solutions suggest that any such structural distortions are similar for both types of micelles.

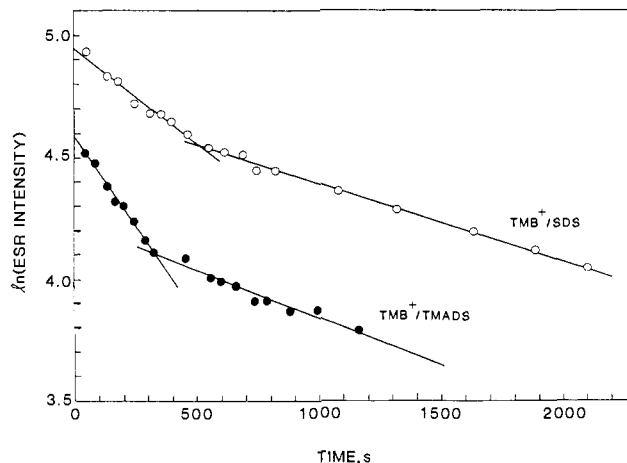


Figure 5. Variation of ESR signal intensity at room temperature of photogenerated TMB<sup>+</sup> after the light source is turned off in TMADS and SDS micelles.

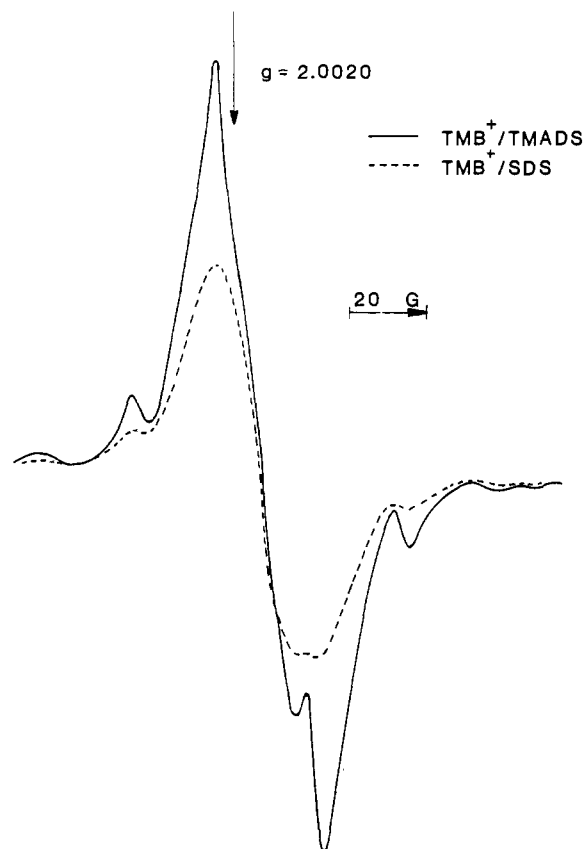


Figure 6. ESR spectra at 77 K of photogenerated TMB<sup>+</sup> in TMADS (—) and SDS (---) micellar solutions; the 370-nm irradiation time was 480 s.

## Discussion

The results indicate that substitution of tetramethylammonium counterion for sodium counterion exerts a significant influence on the structure of dodecyl sulfate micellar solutions which affects the photoionization efficiency of a micellar solubilizate.

The question of water penetration into micelles has been controversial.<sup>10-12</sup> A different approach to this question has been given in this work through the use of a *x*-doxylstearic acid spin probes in micelles and measurement of the nitroxide (doxyl) interaction with deuterons of D<sub>2</sub>O by electron spin echo modulation spectroscopy.

(9) Plonka, A.; Kevan, L. *J. Chem. Phys.* **1984**, *81*, 5023.

(10) Lindman, B.; Wennerström, H. *Top. Curr. Chem.* **1980**, *87*, 1.

(11) Menger, F. M. *Acc. Chem. Res.* **1979**, *12*, 111.

(12) Menger, F. M.; Bonicamp, J. M. *J. Am. Chem. Soc.* **1981**, *103*, 2140.

Even though the TMB<sup>+</sup> and nitroxide probe molecules may distort the local structure of the micelle, the interesting findings here are the comparative differences of these probes in SDS vs. TMADS micelles.

Previous work has suggested that the doxylstearic acid molecules are oriented largely parallel to amphiphilic molecules forming membrane bilayers and micelles with the polar carboxyl group in the polar head-group region of these molecular assemblies.<sup>6,13-17</sup> In SDS micelles prepared in D<sub>2</sub>O the weak to barely detectable deuterium modulation found here for *x*-doxylstearic acid probes as *x* varies from *x* = 5 to *x* = 10 indicates a lack of significant water penetration into these micelles. In general, significant deuterium modulation can only be detected by ESEM for interaction distances less than ~0.6 nm.<sup>8</sup> The distance between three carbons in a trans-configured alkyl chain is ~0.25 nm. Thus for average water penetration no further than the polar head-group region or Stern layer in micelles one would expect weak deuterium modulation for 5-doxyl and perhaps for 7-doxylstearic acid and little beyond that as observed. Of course, the exact configuration of the *x*-doxylstearic acid chain will modify the relevant interaction distances somewhat. On less direct grounds we have suggested previously that there is little water penetration into SDS micelles;<sup>3</sup> this earlier conclusion is supported by the present results.

In contrast to SDS micelles, the *x*-doxylstearic acid spin probes indicate significantly more water penetration into TMADS micelles. The deuterium modulation observed by ESEM is detectable for the 10-doxyl probe and increases smoothly for the 7- and 5-doxyl probes. Thus for a trans chain configuration for the doxylstearic acid one might conclude that water penetrates about as far as the fifth carbon from the polar end of the molecule. Again, the chain configuration might modify this somewhat. However, it is significant to note that the surfactant molecules presumably have a trans chain configuration as suggested by experimental data on the micelle radius.<sup>18</sup>

ESEM results for the TMB cation as a paramagnetic probe are quite consistent with the *x*-doxylstearic acid probe results. The TMB cation-water interactions are distinctly stronger in TMADS micelles compared to SDS micelles.

It seems clear that the surfaces of SDS and TMADS micelles must differ on a molecular level. From previous studies<sup>4</sup> the degree of counterion binding to dodecyl sulfate micelles is about the same

for tetramethylammonium cation as for sodium cation. However, nothing is directly known about the location of these cations with respect to the polar head-group region of the micelles. Our results seem best explained by the postulate that sodium cation is in the outer part of the head-group region so that a relatively compact head-group structure is maintained. Correspondingly, the more hydrophobic tetramethylammonium cation is in the inner part of the head-group region forming spacers between the head groups and creating a less compact head-group structure with increased surface roughness which might be described as a thicker Stern layer. This latter situation would appear to be consistent with more water penetration than in the former as concluded from the ESEM results. This structural picture also seems related to the recent work of Almgren and Swarup,<sup>5</sup> who found that addition of tetraethylammonium chloride and other hydrophobic salts into SDS micellar solutions causes a decrease in the micelle aggregation number from which they concluded that hydrophobic counterions act as spacers between the head groups.

We have found that the photoionization efficiency of TMB is greater in TMADS compared to SDS frozen micellar solutions. This enhanced efficiency correlates with stronger TMB<sup>+</sup>-water interactions which correlation we have suggested previously from different evidence.<sup>3</sup> In the framework of the structural model suggested above the enhanced photoionization efficiency in TMADS micelles can be explained as the result of two factors. First, if the micelle head-group structure is less compact in TMADS micelles the negative surface charge density of the sulfate ions is more diffuse, which decreases the repulsive barrier for the photoejected electron to escape from the micelle. Second, deeper water penetration in the TMADS micelles assists in solvation of the photoejected electron, which promotes charge separation.

At room temperature in solution TMB<sup>+</sup> decays faster in TMADS micelles than in SDS micelles on a second timescale. This decay is presumably due to leakage of TMB<sup>+</sup> out of the micelle and/or to neutralization by an anionic species in a back reaction. In both cases the decay would be promoted by enhanced water penetration into the micelle. Thus the same structural models of SDS and TMADS micelle interfaces explain the differences in the degree of water penetration, in the photoionization efficiency of TMB in frozen solutions, and in the TMB<sup>+</sup> decay in liquid solutions.

**Acknowledgment.** This research was supported by the Department of Energy under Contract DE-AS05-80ER10745. We thank Dr. M. Narayana for obtaining some of the electron spin echo results and for helpful instrumental assistance. R.R.M.J. also thanks the Amoco Production Co. for partial research support.

**Registry No.** 5-Doxylstearic acid, 29545-48-0; 7-doxylstearic acid, 40951-82-4; 10-doxylstearic acid, 50613-98-4; TMB radical cation, 21296-82-2; SDS, 151-21-3; TMADS, 2536-43-8.

(13) Seelig, J.; Limacher, H.; Bader, P. *J. Am. Chem. Soc.* **1972**, *94*, 6364.

(14) Hubbell, W. L.; McConnell, H. H. *Proc. Natl. Acad. Sci. U.S.A.* **1969**, *64*, 20.

(15) Libertini, L. J.; Waggoner, A. S.; Jost, P. C.; Griffith, O. H. *Proc. Natl. Acad. Sci. U.S.A.* **1969**, *64*, 13.

(16) Bales, B. L.; Leon, V. *Biochim. Biophys. Acta* **1978**, *509*, 90.

(17) Jost, P.; Libertini, L. L.; Herbert, V. C. *J. Mol. Biol.* **1971**, *59*, 77.

(18) Missel, P. J.; Mazer, N. A.; Benedek, G. B.; Carey, M. C. *J. Phys. Chem.* **1983**, *87*, 1264.